SUPPLEMENTARY INFORMATION

Polyoxime-Functionalized Magnetic Nanoparticles for Uranium Adsorption with High Selectivity over Vanadium

Meiyun Xu[a], Xiaoli Han [a], Daoben Hua[a,b*]

[a] School of Radiological and Interdisciplinary Sciences (RAD-X) and College of Chemistry, Chemical Engineering and Materials Science, Soochow University, Suzhou 215123, China; correspondence to: dbhua_lab@suda.edu.cn;

[b] Collaborative Innovation Center of Radiological Medicine of Jiangsu Higher Education Institutions, Suzhou 215123, China.

AUTHOR EMAIL ADDRESS:

xumy@suda.edu.cn (M. Xu); hanxiaoli15@163.com (X. Han); dbhua_lab@suda.edu.cn (D. Hua)

CORRESPONDING AUTHOR FOOTNOTE.

Dr. D. Hua

Tel & Fax: (+) 86–512–65883261; E–mail: dbhua_lab@suda.edu.cn

Table of contents

Methods. Thermogravimetric analysis (TGA) was carried out by a Q-50 analyzer (TA instruments) with a heating rate of 20 °C/min under a nitrogen flow. Transmission electron microscopy (TEM) was performed on a Tecnai G2 spirit BioTwin field emission scanning electron microscope. Fourier transform infrared (FTIR) spectra were recorded on a Varian-1000 spectrometer. X-ray photoelectron spectroscopy (XPS) was carried out by an ESCALAB 250Xi spectrometer. The concentration of uranium (VI) was determined by thermo high-resolution inductively coupled plasma mass spectrometry (ICP-MS, Element II).

Synthesis of polyglycerol functionalized magnetic nanoparticles (PGMN)[1]. Mangetic nanoparticles were prepared according to the modified literature method. Briefly, Fe(acac)$_3$ (2.0 g, 5.7 mmol) and triethylene glycol (150 mL, 1.13 mol) were mixed by sonication, then slowly heated to reflux over 3 h. After cooling down, ethyl acetate (100 mL) was added to the mixture. The nanoparticles were collected by centrifugation (20 000 *rpm*, 30 min) and washed with ethyl acetate for 4 times, then dried *in vacuo* to give a blackish solid (560.0 mg).

The synthesized magnetic nanoparticles (300.0 mg) were dispersed in glycidol (30 mL, 0.46 mol), and then bath sonicated for 1 h. The resulting brown dispersion was magnetically stirred at 140 °C under nitrogen for 24 h. After being cooled down to room temperature, the resulting gel was diluted with Milli-Q water (100 mL) by bath sonication till getting a homogeneous dispersion. PGMN was recovered after ultracentrifugation at 20, 000 rpm for 2 h. This washing process was repeated six times to remove free PG. The washed sample was freeze-dried *in vacuo* to give a brown solid (422.8 mg).

Synthesis of polyamidoxime functionalized magnetic nanoparticles (PAMN). 2-Cyanoacetyl chloride was synthesized according to reported method.[2] To a suspension of 2-cyanoacetic acid (2.0 g, 23.5 mmol) in anhydrous CH$_2$Cl$_2$ (80 mL) was slowly added oxalyl chloride (2.2 mL, 25.9 mmol) followed by DMF (36 μL) at 0 °C. The reaction mixture was stirred at room temperature for 3 h, and then the solvent was removed *in vacuo*. 2-cyanoacetyl chloride was used in the next reaction without purification.

The dried PGMN (200.0 mg) was dispersed in 16 mL anhydrous DMF and 6 mL anhydrous Et$_3$N with sonication to get a homogeneous dispersion. The PGMN dispersion was added into a 8 mL

anhydrous DMF solution of 2-cyanoacetyl chloride (2.0 g, 19.3 mmol) at room temperature. Next, the mixture was stirred at room temperature under nitrogen overnight. The resulting mixture was washed with DMF for five times and with H_2O for three times by centrifugation at 4,000 rpm for 20 minutes to remove soluble impurities. The resulting sample was dried *in vacuo* at 50 °C to give a blackish solid PNMN (polynitrile-functionalized magnetic nanoparticles, 106.2 mg).

PNMN (20.0 mg) was dispersed in 6 mL ethanol/H_2O (v:v = 1:1) with sonication. The resulting mixture was added with excess hydroxylamine hydrochloride (200.0 mg, 2.88 mmol), and then stirred vigorously at 70 °C under nitrogen for 24 hours. The mixture was washed with ethanol/H_2O (v:v = 1:1) for five times by centrifugation at 4,000 rpm for 10 minutes. The resulting sample was dried *in vacuo* at 40 °C to give a blackish solid PAMN (polyamidoxime-functionalized magnetic nanoparticles, 15.1 mg).[3]

Conversion ratio. The conversion ratio of esterification was calculated based on the content of hydroxyl groups quantified by O1s XPS. Because the total amount of oxygen has changed during esterification, the conversion of esterification can't be gained from the direct decrease of hydroxyl groups. In order to calculate the conversion ratio, it is assumed that the decrease amount of hydroxyl groups equals to half of increase amount of carbonyl groups.

$$M_F \times C_F^{CO} - M_G \times C_G^{CO} = (M_G \times C_G^{OH} - M_F \times C_F^{CO}) \times 2 \qquad (1)$$

$$R_E = (\frac{M_G \times C_G^{OH} - M_F \times C_F^{OH}}{M_G \times C_G^{OH}}) \times 100\% \qquad (2)$$

where R_E is the hydroxyl consumption. M_F and M_G are the oxygen content of PGMN and PFMN, respectively. C_G^{CO} and C_F^{CO} are the C=O group content of PGMN and PFMN, respectively. C_G^{OH} and C_F^{OH} are the hydroxyl content of PGMN and PFMN, respectively. M_G/M_F can be calculated from Equation (1) and Table S2, and then R_E can be calculated from Equation (2).

The content of oxygen didn't change in oximation, so the conversion of oximation (R_O) can be gained according to Equation (3) and Table S2.

$$R_O = (1 - \frac{C_F^{CO}}{C_O^{CO}}) \times 100\% \qquad (3)$$

where C_F^{CO} and C_O^{CO} are the C=O group content of PFMN and POMN, respectively.

Sorption kinetics. Pseudo-first-order model and pseudo-second-order model are expressed as Equation (1) and (2), respectively.[4, 5]

$$\log(q_e - q_t) = \log q_e - (\frac{k_1}{2.303}) \times t \tag{4}$$

$$\frac{t}{q_t} = \frac{1}{k_2 \times q_e^2} + \frac{t}{q_e} \tag{5}$$

where q_e and q_t (mg/g) are the sorption amount of uranium (VI) at equilibrium time and contact time t (min), respectively. k_1 and k_2 are the pseudo-first-order and pseudo-second-order sorption rate constants, respectively. The simulated results were shown in Fig. S2. k_1 and theoretical q_e values ($q_{e,cal}$) of pseudo-first-order model can be determined from the slope and intercept of linear plot of $\log(q_e -q_t)$ versus t. k_2 and theoretical q_e values ($q_{e,cal}$) of pseudo-second-order model can be obtained from the slope and intercept of linear plot of t/q_t versus t.

Sorption isotherms. The isotherms experiment data were simulated by Langmuir model (3) and Freundlich model (4) to obtain the maximum sorption amounts of uranium (q_{max}).[6] They can be expressed as:

$$\frac{C_e}{q_e} = \frac{1}{q_{max}b} + \frac{C_e}{q_{max}} \tag{6}$$

$$\log q_e = \log K_F + \frac{1}{n} \log C_e \tag{7}$$

where q_e and q_{max} refer to the equilibrium and maximum sorption amounts of uranium (VI), respectively; b (L/mg) is the Langmuir constant about the enthalpy of sorption; C_e (mg/L) is the concentration of uranium (VI) at equilibrium; K_F ($mol^{1-n}L^n/g$) and n are the Freundlich constant, which related to sorption capacity and the intensity of sorption, respectively. The simulated results are shown in Fig. S3.

Table S1. Concentrations of various elements in testing solution.[7, 8]

Element	Conc. in typical seawater (ppb)		Total valence ions	Simulated seawater conc. in testing solution (ppb)
	average	range		
U	3.3		$UO_2(CO_3)_3^{4-}$, $UO_2(CO_3)_2^{2-}$	251.0
V	1.65	1.5-2.5	$VO_2(OH)_3^{2-}$ VO_3^-, HVO_4^{2-} $H_2VO_4^-$	137.8
Cr	0.05	0.04-0.07	CrO_4^{2-}	23.9
Co	0.032	<0.005-0.092	Co^{2+}	184.6
Ni	1.7	0.8-2.4	Ni^+	81.9
Cu	0.7	0.2-4.0	Cu^{2+}	477.6
Zn	2	1-8	Zn^{2+}	89.1
Cd	0.113	0.02-0.25	$CdCl^+$, $CdCl_3^-$, Cd^{2+}	259.9

Table S2. The contents of different functional groups calculated from XPS O1s spectra.

Materials	Peak	Binding energy (eV)	FWHM[*] (eV)	Content of oxygen moiety (%)
PGMN	C-O-H	533.2	1.60	41.6
	C-O-C	532.3	1.28	53.9
	C=O	531.8	0.58	4.5
PFMN	C-O-H	533.4	1.58	21.2
	C-O-C	532.6	1.25	50.3
	C=O	532.0	1.10	28.5
POMN	N(C)-O-H	533.3	1.30	25.9
	C-O-C	532.8	1.10	49.2
	C=O	532.1	1.30	17.1
	O^{2-}	530.1	1.18	7.8
POMN-U(VI)	N(C)-O---U	533.8	0.90	3.7
	C-O-H, C=O---U	533.2	1.00	20.1
	C-O-C	532.6	1.20	50.8
	C=O	532.0	0.50	4.1
	N(C)-O-U	531.4	1.13	15.5
	O^{2-}	530.3	1.11	5.8

[*]: Full width at half maximum.

Table S3. Kinetic parameters for uranium sorption on POMN.

Sorbent		Pseudo-first-order			Pseudo-second-order		
	$q_{e,exp}$	k_1	$q_{e,cal}$	R^2	k_2	$q_{e,cal}$	R^2
	(mg/g)	(min^{-1})	(mg/g)		(g/min/mg)	(mg/g)	
POMN	3.996	0.006	0.172	0	2.199	3.893	1.000

Table S4. Langmuir and Freundlich parameters for uranium (VI) sorption on POMN.

Sorbent	Langmiur model			Freundlich model		
	$q_{max,cal}$	b	R^2	K_F	n	R^2
	(mg/g)	(L/mg)		(mol^{1-n} L^n/g)		
PGMN	105.6	0.059	0.996	8.396	1.603	0.991
PFMN	159.2	0.578	0.989	61.62	3.675	0.914
POMN	141.4	0.482	0.992	41.64	2.487	0.911

Table S5. The contents of different functional groups calculated from N 1s spectra.

Materials	Peak	Binding energy (eV)	FWHM* (eV)	%
POMN	1	400.6	1.01	100
POMN-U(VI)	1	401.2	3.50	81.8
	2	399.7	0.90	18.2

*: Full width at half maximum.

η^2 binding, 0.34 kcal/mol   Five-coordinate uranyl complex, 3.48 kcal/mol
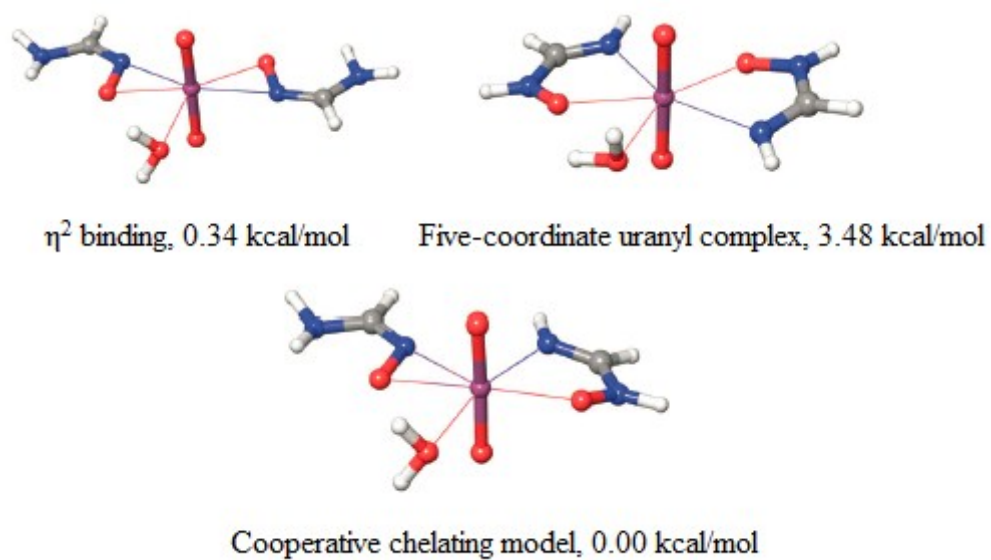
Cooperative chelating model, 0.00 kcal/mol

Fig. S1 Structures of uranyl complexes with formamidoxime obtained after geometry optimization at the B3LYP/SSC/6-311++G(d,p) level of theory.[9]
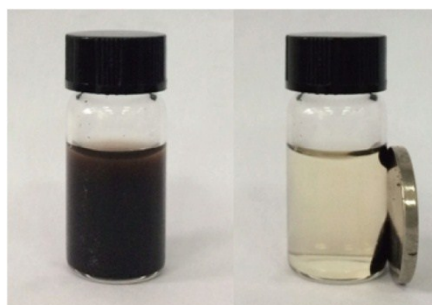

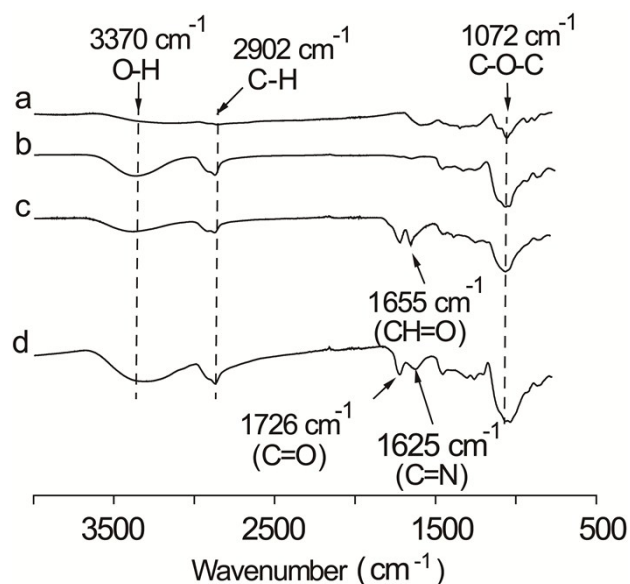Fig. S2 Water dispersion of POMN and magnetic separation.

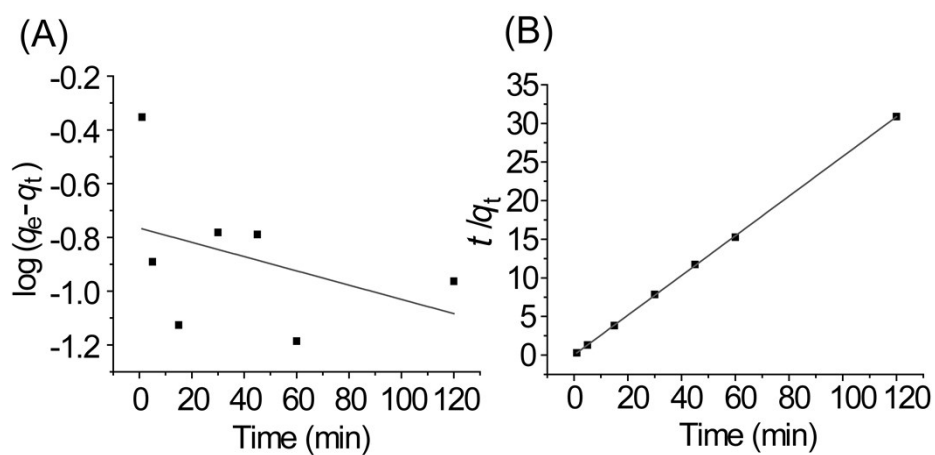Fig. S3 Full FTIR spectra of (a) MN, (b) PGMN, (c) PFMN, and (d) POMN.

Fig. S4 (A) Pseudo-first order kinetics and (B) Pseudo-second order kinetics of uranium (VI) sorption on POMN. (Experiment condition: $C_{U\ initial}$ = 0.01 mmol/L, $C_{sorbent}$ = 0.5 mg/mL, pH 8.0±0.1, and 298.15 K)
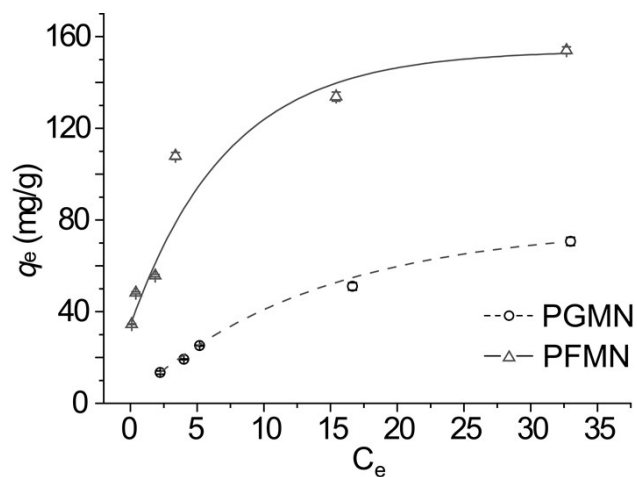
Fig. S5 Isotherms of uranium (VI) sorption on PGMN and PFMN. (Experiment condition: $C_{U\ initial}$ = 0.01 mmol/L, $C_{sorbent}$ = 0.5 mg/mL, pH 8.0±0.1, and 298.15 K)
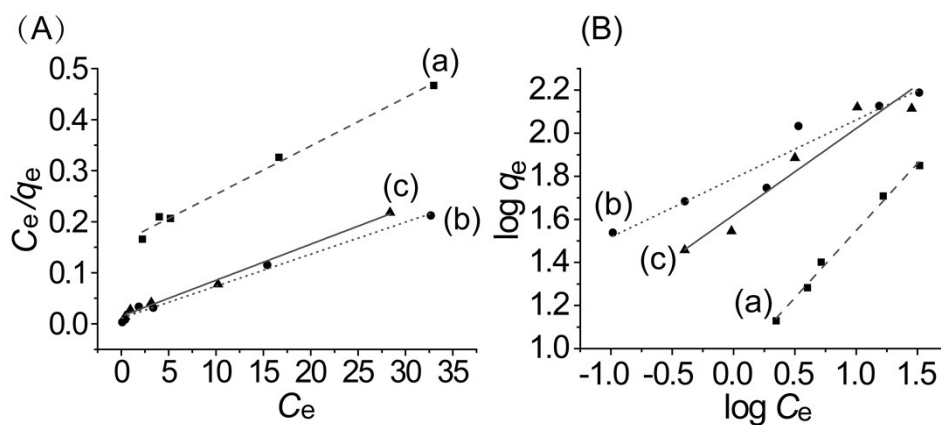
Fig. S6 (A) Langmuir model and (B) Freundlich model of uranium (VI) sorption on (a) PGMN, (b) PFMN and (c) POMN. (Experiment condition: $C_{U\ initial}$ = 0.01 mmol/L, $C_{sorbent}$ = 0.5 mg/mL, pH 8.0±0.1, and 298.15 K)
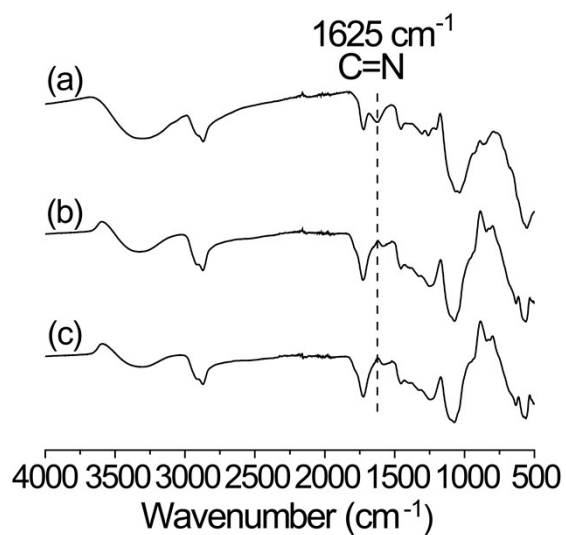
Fig. S7 FTIR spectra of POMN (a) before and after elution with (b) 0.01 M HCl and (c) 0.1 M HCl. (Experiment condition: $C_{U\ initial}$ = 0.01 mmol/L, $C_{V\ initial}$ = 0.01 mmol/L, $C_{sorbent}$ = 0.5 mg/mL, pH 8.0±0.1, and 298.15 K)
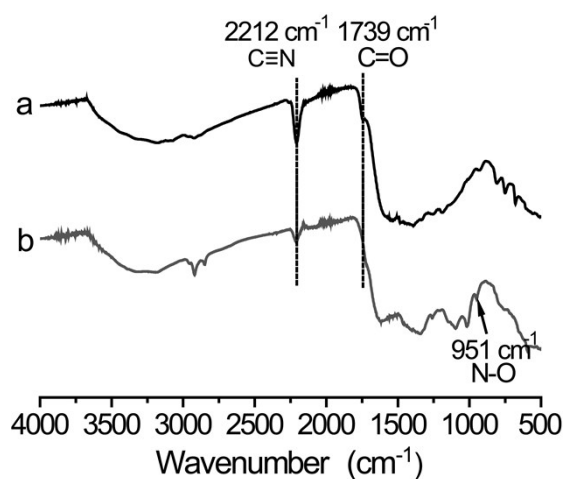

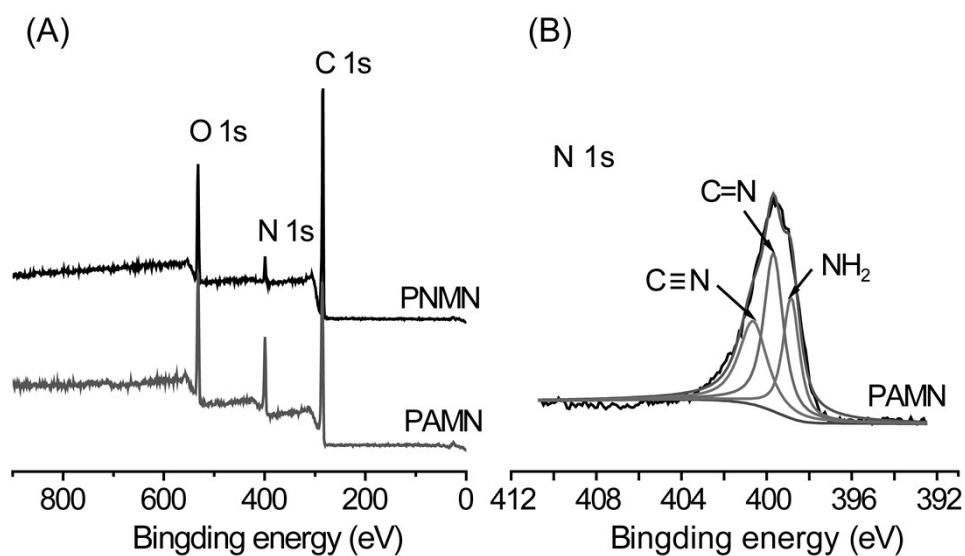Fig. S8 FTIR spectra of (a) PNMN and (b) PAMN.

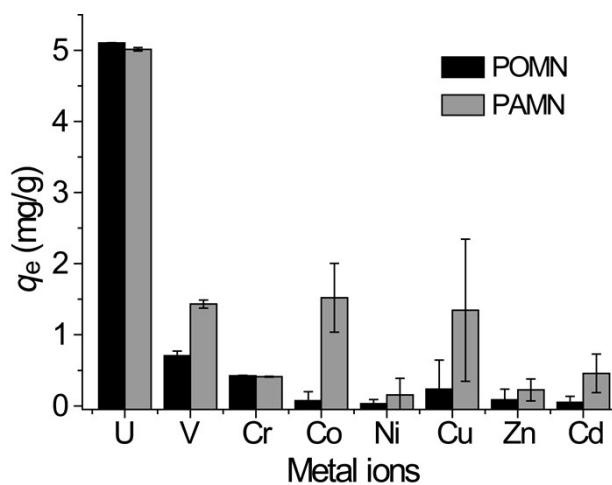Fig. S9 XPS survey scan of PAMN and PNMN (A), XPS N 1s spectra of PAMN (B).

Fig. S10 Uptake capacity of POMN and PAMN for metal ions in simulated seawater. (Experimental conditions: $C_{sorbent}$ = 0.05 mg/mL, pH 8.0±0.1, and 298.15 K, every sample contained 7.0 g sea salt in 200 mL Milli-Q water)

Reference

1. L. Zhao, T. Chano, S. Morikawa, Y. Saito, A. Shiino, S. Shimizu, T. Maeda, T. Irie, S. Aonuma, H. Okabe, T. Kimura, T. Inubushi and N. Komatsu, *Advanced Functional Materials*, 2012, **22**, 5107-5117.

2. S. Mo, X. Li and J. Xu, *The Journal of Organic Chemistry*, 2014, **79**, 9186-9195.

3. Z. Zeng, Y. Wei, L. Shen and D. Hua, *Industrial & Engineering Chemistry Research*, 2015, **54**, 8699-8705.

4. Y. S. Ho and G. McKay, *Process Biochemistry*, 1999, **34**, 451-465.

5. Y. S. Ho and G. McKay, *Water Research*, 2000, **34**, 735-742.

6. S. Sadeghi and E. Aboobakri, *Microchimica Acta*, 2012, **178**, 89-97.

7. S. Xie, X. Liu, B. Zhang, H. Ma, C. Ling, M. Yu, L. Li and J. Li, *Journal of Materials Chemistry A*, 2015, **3**, 2552-2558.

8. J. Hu, H. Ma, Z. Xing, X. Liu, L. Xu, R. Li, C. Lin, M. Wang, J. Li and G. Wu, *Industrial & Engineering Chemistry Research*, 2016, **55**, 4118-4124.

9. S. T. Tsantis, E. Zagoraiou, A. Savvidou, C. P. Raptopoulou, V. Psycharis, L. Szyrwiel, M. Holynska and S. P. Perlepes, *Dalton Transactions*, 2016, **45**, 9307-9319.